International Journal of Transport Development and Integration
Vol. 8, No. 4, December, 2024, pp. 497-504
Journal homepage: http://iieta.org/journals/ijtdi

Mathematical Model for Sizing and Optimizing a Test Bench for Electric Motors of Electric Vehicles

Emiliano Lustrissimi[1*], Bonifacio Bianco[2], Sebastiano Caravaggi[2], Antonio Rosato[1]

[1] Department of Architecture and Industrial Design, University of Campania Luigi Vanvitelli, Aversa 81031, Italy
[2] Assing S.p.A., Monterotondo 00015, Italy

Corresponding Author Email: emiliano.lustrissimi@unicampania.it

https://doi.org/10.18280/ijtdi.080401

Received: 26 June 2024
Revised: 28 October 2024
Accepted: 13 November 2024
Available online: 26 December 2024

Keywords:
electric vehicles, end-of-production-line test bench, mathematical model, field test, energy consumption saving

ABSTRACT

A mathematical model has been formulated to optimize the setup of an end-of-production-line (EOL) test bench that is used to evaluate the efficiency of electric motors or axles designed for electric vehicles. The model can forecast the performance of EOL testing benches and electric motors/axles under a variety of conditions, thereby eliminating the need for extensive physical trials and minimizing the associated energy usage. The proposed model can be adjusted to handle different power ratings of electric motors or axles. The model takes the maximum performance that the electric motors or axles need to guarantee according to the vehicle manufacturer's specifications as inputs. Subsequently, the necessary performance of each primary EOL test bench component is computed, and the corresponding systems available in the market are chosen based on manufacturers' catalogues. In this research, an EOL test bench for low-power e-axles (approximately 22 kW) has been designed according to the outputs of the proposed model.

1. INTRODUCTION

In the current context, where environmental considerations are driving technological advancements, electric vehicles (EVs) [1, 2] have become a crucial area of research across various industries. One of the key components of these vehicles is the electric machines (EMs) [3, 4]. EMs form the heart of the EVs' powertrain, responsible for generating the necessary torque and power to propel the vehicle's wheels by transforming electrical energy into mechanical energy. It is essential to conduct proper testing, evaluation, and validation to fully harness the energy conversion potential of these advanced powertrains [5-8], leading to significant modifications in the structure of manufacturing facilities.

An end-of-production-line (EOL) test bench is a dedicated setup or platform designed to assess, evaluate, and validate the performance, functionality, and reliability of a system or component. These EOL test benches are positioned at the end of the production line to conduct various functional tests to verify the compliance of the newly produced components with the design specifications. These benches often need to be incorporated into production lines and align with new Industry 4.0 approaches [9], focusing on eco-sustainability and integration with other systems to optimize all plant processes. The design of EOL test benches is crucial to leverage the benefits brought by EMs; however, this design has been challenging due to the multitude of design variables and the multidisciplinary nature of the subject [10-13]. The components of these EOL test benches, such as the test dynamometers connected via drive shafts, which are responsible for decelerating or accelerating the EMs to execute the required test cycle, are characterized by the highest power consumption.

The design of EOL test benches can be enhanced by implementing specially developed mathematical models capable of simulating and predicting the behaviour of the EMs under various boundary conditions, thereby eliminating the need for extensive field testing. Assing S.p.A. [14] has designed and built an electric motor EOL test bench for testing a low-power electric axle (approximately 22 kW) with a maximum voltage of 52 V and a maximum EM rotational speed of about 20000 rpm. Furthermore, a mathematical model has been developed to design the electric axle EOL test bench, aiming to reduce the corresponding power consumption and ensure the maximum performance of the tested device under the selected test conditions.

2. DESCRIPTION OF AN EOL BENCH FOR ELECTRIC MOTORS AND AXLES

In the field of automobile manufacturing, there are primarily two categories of test benches: the first type is used for testing electric motors [1], while the second type is utilized for testing electric axles (e-axle) [6] (that is essentially an electric motor coupled with a gearbox). The first category of test benches is known for their high rotational speeds (with some of the newer models reaching up to 25000 rpm) and low torques. On the other hand, the latter category is characterized by their low rotational speeds (approximately in the range of

thousands of rpm) and high torques, as they are directly linked to the wheels of the vehicle.

Another significant difference between the two categories of test benches relates to the number of dynamometers required for testing: in the case of electric axles, two dynamometers are needed, whereas a single dynamometer is adequate for testing electric motors. However, the dynamometer used for testing electric motors is more costly if compared with the two dynamometers used for electric axles due to its higher rotational speed, which necessitates greater stress resistance, more expensive materials, and more precise controls of high-frequency currents.

Besides the dynamometers and the base structure, a test bench includes several other essential components such as: a data acquisition system (DAQ), a human-machine interface (HMI), a programmable logic controller (PLC), a cooling system, a panel for air and fluid distribution, an electrical cabinet, and a dynamometer transmission. As shown in Figure 1, these components are arranged around the test bench to maximize space efficiency, while still ensuring enough clearance for safe maintenance operations.

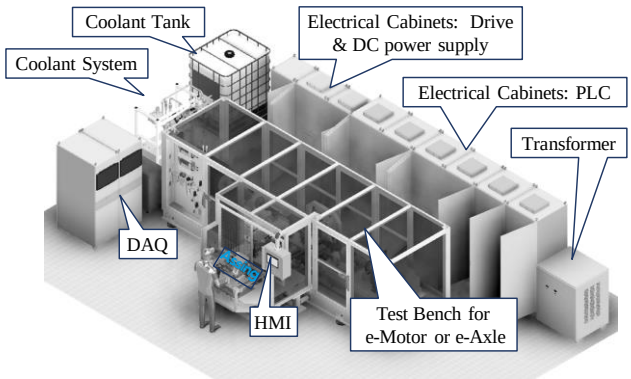

Figure 1. Main components of EOL test benches

The data acquisition (DAQ) system serves as the interface with the plant's data exchange system, facilitating the exchange of information about the components under testing, setting the suitable cycle for them, managing the active bench and area safety measures, capturing various measurements, and evaluating the results to verify component's compliance.

The operator communicates with the programmable logic controller (PLC) via the human-machine interface (HMI). The PLC supervises all mechanical, electrical, and fluidic actuations and safety components (such as alarms, closed doors, secured component positions, the operator's position relative to the test area), granting the operator control over the test area. The bench's cooling system comprises a coolant distribution system and a coolant tank. The distribution system, made up of pipes, valves, and pumps, is engineered to supply the correct coolant flow to each bench component (typically the system under test, dynamometers, inverters, and electrical panels). Some benches include a mixing component that pulls water from the building and mixes it with glycol in ratios specified by the customer.

Electrical cabinets are designed to accommodate all electrical equipment, enabling their interconnection, cooling, and protecting operators from the risks associated with high voltages and currents. They usually house the drives (inverters) that control the dynamometers to simulate road load and various test cycles, the battery emulator or DC power supply that powers the EM during testing by emulating the vehicle battery, and the 24 V and 12 V power supply for various bench utilities. All electrical components can be connected to a common line, which can be either AC or DC. If the DC link solution is selected for connecting the bench to the grid, an active front end (AFE) system is needed to convert from AC to DC. This system specifically includes two parts: a first part for converting from AC to DC (known as active line module (ALM)) and a second part to rephase the current output from the bench and prevent disturbances on the plant line (known as active interface module (AIM)).

Figures 2 and 3 illustrate the electrical connections between the main power components in both the link configurations. Specifically, Figure 2 pertains to the DC one where all electrical components are powered in common through a DC connection, but this requires a common AFE to be connected to the grid. Conversely, Figure 3 depicts the connection between the same components but in this case directly to AC, without the need to incorporate an AFE to connect to the plant network.

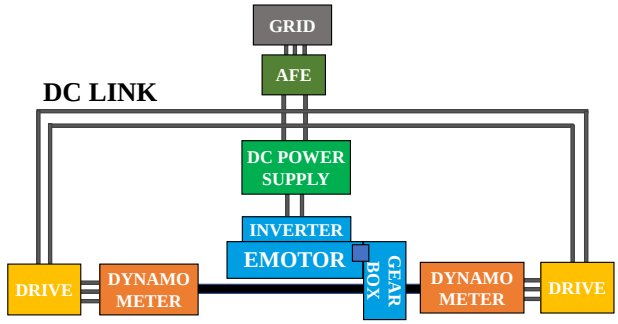

Figure 2. Connection diagram of the electrical power components of the bench in the case of DC link configuration

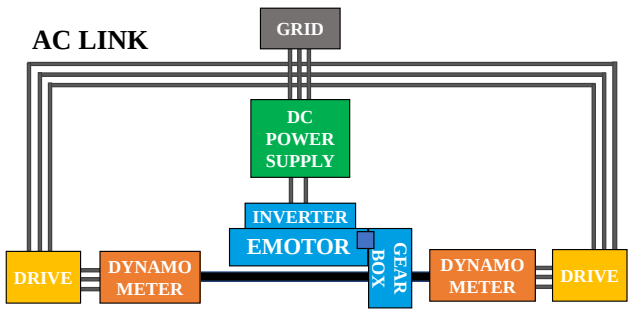

Figure 3. Connection diagram of the electrical power components of the bench in the case of AC link configuration

The final elements to be examined are those composing the transmissions. These elements link the dynamometers to the output of the device under testing, simulating the required test conditions. These conditions are often supplied by the car manufacturer in the form of torque and speed profiles as a function of the test duration.

The design of these components is especially crucial for testing electric motors, where high rotations, even with slight eccentricities, can lead to disastrous failures. The primary components of the drivelines include the torque transducer, which measures the applied torque and dynamometer revolutions, the torque limiter that limits the applied torque values in case of a failure, the half-shaft that connects with the device under test and enables torque transfer, and the spindle, which compensates for any misalignment between the dynamometer and the points of engagement of the half-shaft.

Figure 4 shows the arrangement of the main components that make up the driveline.

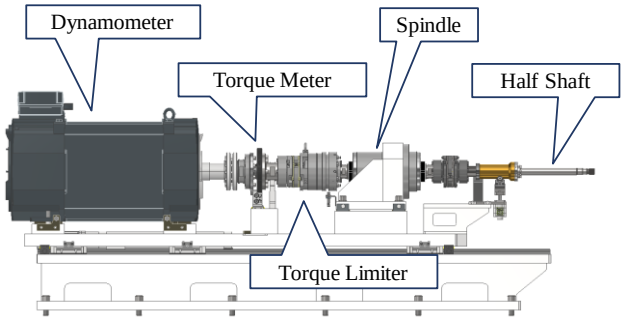

Figure 4. Driveline main components

Numerous companies, such as Assing S.p.A. [14], design and construct end-of-line (EOL) test benches to evaluate electric motors and e-axles produced by leading automotive manufacturers. These EOL test benches are vital as they enable the assessment of the performance and behaviour of various components manufactured along the production line. However, their operation is characterized by substantial electrical consumption, making their accurate sizing crucial with respect to the total energy consumption of the manufacturing plant.

The impact of proper component sizing on energy usage can be examined using a bench configured for testing a 20 kW electric motor by assuming a 90% operational availability and a production cycle of 180 seconds. Considering that the average power output during testing is 25% of the motor's maximum capacity, a conventional design strategy involving energy dissipation results in an estimated annual energy consumption of 49.3 MWh. However, a green approach that incorporates new technologies for recycling internal energy can reduce this to approximately 15.7 MWh per year. This underscores the potential of green strategies in decreasing energy requirements.

The sizing of EOL test benches depends on several factors; some factors relate to the device under test (DUT) itself, such as performance curves and desired test conditions specified by the electric vehicle/axle manufacturer; some other factors are linked to the components that constitute the bench, including market availability and power ratings suitable for the DUT. Therefore, a mathematical model that appropriately sizes EOL test benches based on the automaker's requirements, ideally minimizing electrical energy consumption, is fundamentally important.

3. EOL TEST BENCH MODEL DESIGN

In this research, a mathematical model has been formulated to determine the sizing of end-of-line (EOL) test benches. These benches have to be installed at the end of the production line in automotive companies' plants for the purpose of testing e-axles.

The model necessitates the following initial inputs:

1) E-axle maximum torque: $T_{M\text{-}EM}$;

2) E-axle maximum revolution speed at maximum torque: $n_{B\text{-}EM}$;

3) E-axle maximum revolution speed: $n_{M\text{-}EM}$;

4) E-axle maximum power: $P_{M\text{-}EM}$;

5) E-axle maximum revolution speed variation: $\dot{\omega}_{M-EM}$.

For each specific e-axle model, the automotive manufacturer provides to EOL test bench supplier companies (such as Assing S.p.A. [14]) a performance map including the two curves:

- The first curve represents the power as a function of the half-shaft speed. This curve allows to define the maximum power value that can be delivered for up to 10 seconds;
- The second curve represents the torque as a function of the half-shaft speed. This curve indicates the maximum torque values that can be delivered for up to 10 seconds.

Figure 5 illustrates a typical example of these two curves, from which the first four model inputs can be derived.

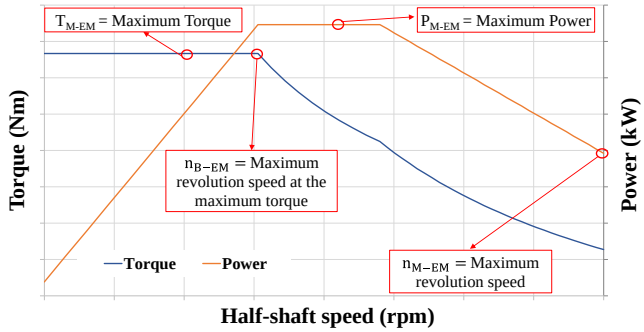

Figure 5. Example of performance curves provided by automotive companies with reference to a generic e-axle model

The fifth input of the model is determined based on a specific cycle outlined by the automotive manufacturer producing the e-axle under analysis. This cycle represents the rotational speed as a function of time that the manufacturer would like to apply to the e-axle. Figure 6 depicts a typical example of such a cycle. Starting from this curve, the point corresponding to the maximum derivative (and, therefore, the maximum variation of rotational speed) is selected.

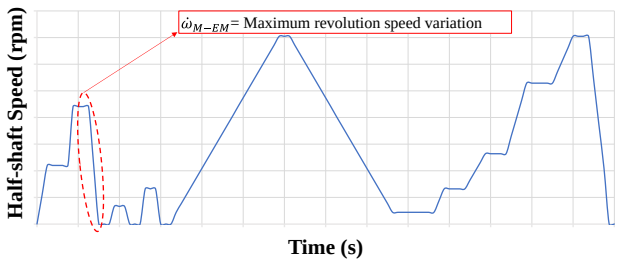

Figure 6. Example of a typical e-axle test cycle

Once all the 5 inputs are defined, the proposed model allows to obtain the following outputs:

- Dynamometer maximum torque: $T_{M\text{-}DY}$;
- Dynamometer maximum power: $P_{M\text{-}DY}$;
- Dynamometer maximum rotational speed: $n_{M\text{-}DY}$.

Using $\dot{\omega}_{M-EM}$ and the inertia total moment of the system I_T, the inertial contribution in terms of torque $T_{T\text{-}I}$ can be calculated, so it possible to evaluate the dynamometer maximum torque $T_{M\text{-}DY}$:

$$T_{T\text{-}I} = I_T \cdot \dot{\omega}_{M\text{-}EM} \quad (1)$$

$$T_{M\text{-}DY} = T_{M\text{-}EM} + T_{T\text{-}I} \quad (2)$$

With the maximum torque value of the dynamometer and considering the maximum revolution speed at maximum torque, it is possible to calculate the maximum power required to the dynamometer $P_{M\text{-}DY}$:

$$P_{M\text{-}DY} = T_{M\text{-}DY} \cdot n_{B\text{-}EM} \tag{3}$$

Selecting a dynamo with the same maximum speed as the electric axle does not ensure optimal system control at extreme points. Therefore, a dynamometer is typically chosen with a maximum revolution speed that is at least 10% higher than that of the axle ($n_{M\text{-}DY}$):

$$n_{M\text{-}DY} = 1.1 \cdot n_{B\text{-}EM} \tag{4}$$

Based on the previous outputs calculated by using Eqs. (1)-(4), the models of the dynamometers can be manually chosen according to the performance stated by the manufacturers in their respective catalogues. Once the models of the dynamometers are selected, the following parameters can be derived from the manufacturers' catalogues:

- Pole pairs number: C_p;
- Dynamometers efficiency: η_{DY};
- Dynamometer supply voltage: V_{DY};
- Power factor: $\cos\varphi_{DY}$.

Once the previous information is obtained for the selected models of the dynamometers, the subsequent electrical parameters associated with the drives are calculated:

- Switching frequency: f_M;
- Maximum output drive active power: $P_{M\text{-}O\text{-}D}$;
- Maximum output drive current: $I_{M\text{-}O\text{-}D}$;
- Maximum output drive apparent power: $A_{M\text{-}O\text{-}D}$.

The corresponding calculation is performed by means of the following Eqs. (5)-(8):

$$f_M = \frac{n_{M-DY} \cdot C_P}{60} \tag{5}$$

$$P_{M\text{-}O\text{-}D} = \frac{P_{M\text{-}DY}}{\eta_{DY}} \tag{6}$$

$$I_{M\text{-}O\text{-}D} = \frac{P_{M\text{-}O\text{-}D}}{\sqrt{3} \cdot \cos\varphi_{DY} \cdot V_{DY}} \tag{7}$$

$$A_{M\text{-}O\text{-}D} = \frac{P_{M\text{-}O\text{-}D}}{\cos\varphi_{DY}} \tag{8}$$

Once the previous parameters are calculated, a manual selection is made from the manufacturer's catalogues of the drives. These drives are characterized by performance aligning with the values of the parameters calculated by using Eqs. (5)-(8). Taking into account costs, performance, and delivery time, it is possible to select either DC drives or AC drives that best match the calculated parameters. Specifically, the following performance data are derived from the technical catalogues of the drives:

- Power factor $\cos\varphi_D$ for AC link connection;
- Drive efficiency $\eta_{AC\text{-}D}$ for AC link connection;
- Drive AC supply voltage $V_{AC\text{-}S\text{-}D}$ for AC link connection;
- Drive efficiency $\eta_{DC\text{-}D}$ for DC link connection;
- Drive DC supply voltage $V_{DC\text{-}S\text{-}D}$ for DC link connection.

Based on the selected link type, it is possible to calculate the following parameters:

- Maximum AC supply drive active power $P_{M\text{-}S\text{-}D_{AC}}$ for AC link connection;
- Maximum AC supply drive current $I_{M\text{-}S\text{-}D_{AC}}$ for AC link connection;
- Maximum AC supply drive apparent power $A_{M\text{-}S\text{-}D_{AC}}$ for AC link connection;
- Maximum DC supply drive power $P_{M\text{-}S\text{-}D_{DC}}$ for DC link connection;
- Maximum DC supply drive current $I_{M\text{-}S\text{-}D_{DC}}$ for DC link connection.

The following Eqs. (9)-(13) are used for calculating the previous parameters:

$$P_{M\text{-}S\text{-}D_{AC}} = \frac{P_{M\text{-}O\text{-}D}}{\eta_{AC-D}} \tag{9}$$

$$I_{M\text{-}S\text{-}D_{AC}} = \frac{P_{M\text{-}S\text{-}D_{AC}}}{\sqrt{3} \cdot \cos\varphi_D \cdot V_{AC\text{-}S\text{-}D}} \tag{10}$$

$$A_{M\text{-}S\text{-}D_{AC}} = \frac{P_{M\text{-}S\text{-}D_{AC}}}{\cos\varphi_D} \tag{11}$$

$$P_{M\text{-}S\text{-}D_{DC}} = \frac{P_{M\text{-}O\text{-}D}}{\eta_{DC-D}} \tag{12}$$

$$I_{M\text{-}S\text{-}D_{DC}} = \frac{P_{M\text{-}S\text{-}D_{DC}}}{V_{DC\text{-}S\text{-}D}} \tag{13}$$

Figure 7 presents the flowchart for using the drive branch sizing model with the steps previously discussed. Once the calculations of the main parameters and the selection of components on the dynamo branch are completed, it is possible to apply the same procedure to the DC power (DCP) supply branch.

The maximum power of the e-axle $P_{M\text{-}EM}$ can be determined from Figure 5, after which the maximum e-axle supply power $P_{M\text{-}O\text{-}DCP}$ and the maximum e-axle supply current $I_{M\text{-}O\text{-}DCP}$ can be computed via the following Eqs. (14)-(15):

$$P_{M\text{-}O-DCP} = \frac{P_{M\text{-}EM}}{\eta_{GB} \cdot \eta_{EM} \cdot \eta_I} \tag{14}$$

$$I_{M\text{-}O-DCP} = \frac{P_{M\text{-}O-DCP}}{V_{EM-DC}} \tag{15}$$

where, η_{GB}, η_{EM}, η_I, and $V_{EM\text{-}DC}$ stand for gearbox efficiency, EM efficiency, inverter efficiency, and nominal test supply voltage (the car makers define these characteristics at the start of the project).

Regarding the drive selection, after utilizing Eqs. (14)-(15) to evaluate the input parameter values, an alternative common link power supply can be chosen. The following parameters are obtained from technical datasheets provided by manufacturers:

- Power factor $\cos\varphi_{DCP}$ for AC link connection;
- DCP efficiency $\eta_{AC\text{-}DCP}$ for AC link connection;

• DCP AC supply voltage $V_{AC\text{-}S\text{-}DCP}$ for AC link connection;
• DCP efficiency $\eta_{DC\text{-}DCP}$ for DC link connection;
• DCP DC supply voltage $V_{DC\text{-}S\text{-}DCP}$ for DC link connection.

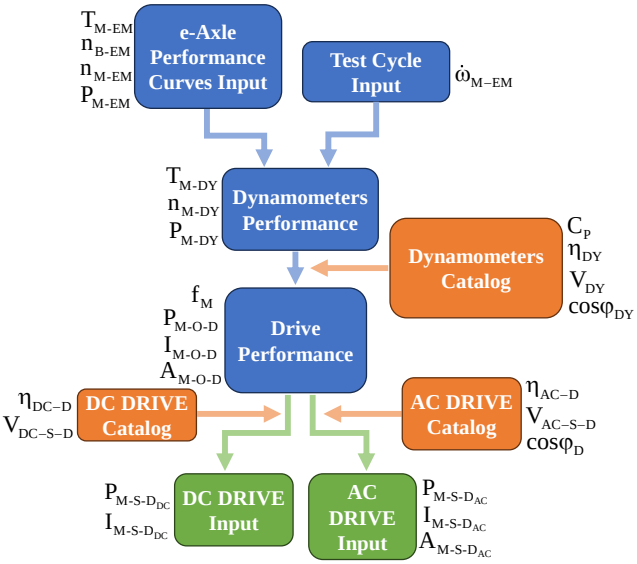

Figure 7. Flowchart of the procedure for drive branch sizing model

Based on the link type selected, it is possible to calculate the following DCP input parameters via Eqs. (16)-(20):

• Maximum AC supply DCP active power $P_{M\text{-}S\text{-}DCP_{AC}}$ for AC link connection;
• Maximum AC supply DCP current $I_{M\text{-}S\text{-}DCP_{AC}}$ for AC link connection;
• Maximum AC supply DCP apparent power $A_{M\text{-}S\text{-}DCP_{AC}}$ for AC link connection;
• Maximum DC supply DCP power $P_{M\text{-}S\text{-}DCP_{DC}}$ for DC link connection;
• Maximum DC supply DCP current $I_{M\text{-}S\text{-}DCP_{DC}}$ for DC link connection.

$$P_{M\text{-}S\text{-}DCP_{AC}} = \frac{P_{M\text{-}O\text{-}DCP}}{\eta_{AC-DCP}} \tag{16}$$

$$I_{M\text{-}S\text{-}DCP_{AC}} = \frac{P_{M\text{-}S\text{-}DCP_{AC}}}{\sqrt{3}\cdot\cos\varphi_{DCP}\cdot V_{AC\text{-}S\text{-}DCP}} \tag{17}$$

$$A_{M\text{-}S\text{-}DCP_{AC}} = \frac{P_{M\text{-}S\text{-}DCP_{AC}}}{\cos\varphi_{DCP}} \tag{18}$$

$$P_{M\text{-}S\text{-}DCP_{DC}} = \frac{P_{M\text{-}O\text{-}DCP}}{\eta_{DC-DCP}} \tag{19}$$

$$I_{M\text{-}S\text{-}DCP_{DC}} = \frac{P_{M\text{-}S\text{-}DCP_{DC}}}{V_{DC\text{-}S\text{-}DCP}} \tag{20}$$

The flowchart synthesizing the DCP branch sizing model using the previously described procedures is shown in Figure 8.

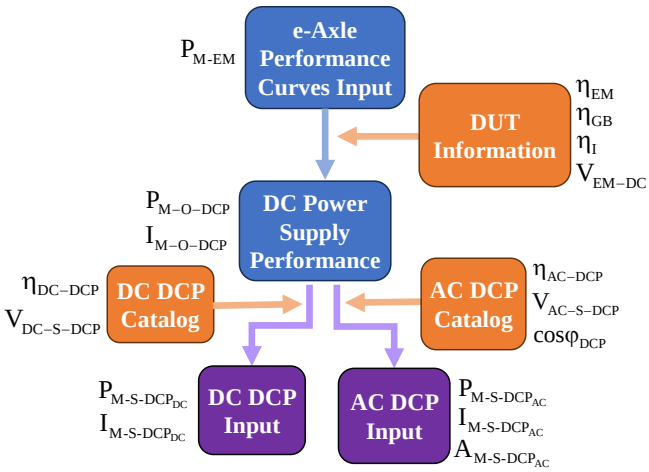

Figure 8. DCP branch sizing flowchart

As previously indicated, the test bench needs an additional component to be sized in the case of a DC link. The maximum DC output power $P_{M\text{-}O\text{-}AFE}$ of the AFE and the maximum DC output current $I_{M\text{-}O\text{-}AFE}$ of the AFE are calculated as follows:

$$P_{M\text{-}O\text{-}AFE} = \text{maximum}(P_{M\text{-}S\text{-}D_{DC}}, P_{M\text{-}S\text{-}DCP_{DC}}) \tag{21}$$

$$I_{M\text{-}O\text{-}AFE} = \text{maximum}(I_{M\text{-}S\text{-}D_{DC}}, I_{M\text{-}S\text{-}DCP_{DC}}) \tag{22}$$

To precisely determine its sizes and the necessary performance metrics, the highest values among those asked for as inputs on one of the two branches (drive branch, DCP branch) are selected. Because the powers exchanged between the two branches during normal operation partially compensate each other, this strategy assures power coverage at all operational points. As a result, the AFE power requirements will undoubtedly be lower than the maximum power that can be supplied.

It is feasible to choose the suitable AFE using these characteristics. Consequently, the manufacturer's data found in the corresponding catalogues can be used to generate the following parameters:

• AFE power factor: $\cos\varphi_{AFE}$;
• AFE efficiency: η_{AFE};
• Plant supply voltage: V_{PLANT}.

With these parameters, it is possible to calculate the maximum electrical input to the test bench from the power line of the plant:

• Maximum supply AFE active power: $P_{M\text{-}S\text{-}AFE}$;
• Maximum supply AFE current: $I_{M\text{-}S\text{-}AFE}$;
• Maximum supply AFE apparent power: $A_{M\text{-}S\text{-}AFE}$.

The following equations are used for calculating the previous parameters:

$$P_{M\text{-}S\text{-}AFE} = \frac{P_{M\text{-}O\text{-}AFE}}{\eta_{AFE}} \tag{23}$$

$$I_{M\text{-}S\text{-}AFE} = \frac{P_{M\text{-}S\text{-}AFE}}{\sqrt{3}\cdot\cos\varphi_{AFE}\cdot V_{PLANT}} \tag{24}$$

$$A_{M\text{-}S\text{-}AFE} = \frac{P_{M\text{-}S\text{-}AFE}}{\cos\varphi_{AFE}} \tag{25}$$

4. EOL TEST BENCH MODEL RESULTS

The proposed model has been used to design an EOL test bench for testing an e-axle with nominal voltage supply of 48 V and total power of approximately 22 kW.

Based on the manufacturer's data, Figure 9 displays torque and power of the e-axle under analysis as a function of each half-shaft's rotating speed.

The following first four inputs needed by the model (shown in Figure 5) can be obtained from Figure 9:

1) $T_{M\text{-}EM}$ = 1022 Nm;
2) $n_{B\text{-}EM}$ = 103 Nm;
3) $n_{M\text{-}EM}$ = 872 rpm;
4) $P_{M\text{-}EM}$ = 11 kW.

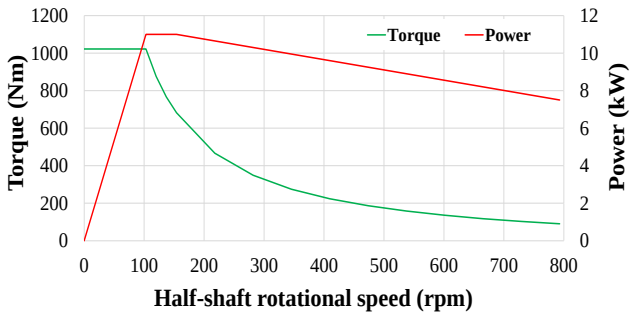

Figure 9. Torque and power of the electric axle under investigation as a function of the rotational speed of each half-shaft according to manufacturer data

Figure 10 shows the test profiles defined by the car manufacturer, reporting the torque and revolution speed to be followed by the e-axle during the test. In particular, from the reported revolution speed profile it is possible to derive the fifth input of the model $\dot{\omega}_{M-EM}$ (shown in Figure 6) which is equal to 105 rpm/s.

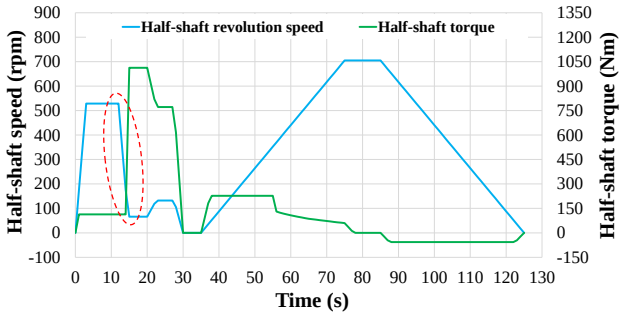

Figure 10. Cycle test torque and speed profiles

The manufacturer necessitates a specific and exact control over the e-axle's 48 V power supply. Given the substantial voltage difference between the e-axle and the rest of the bench's electrical components, which surpassed 400 V, a hybrid solution was put into place. This solution, as shown in Figure 11, involved a DC link and an AC link. In particular, the AC Link includes 2 dynamometers (model 1PH8226-1DB20-0LA1 [15]), 2 drives (model 6SL3120-1TE32-0AA4 [16]), AFE-ALM (model 6SL3330-7TE32-6AA3 [16]), and AFE-AIM (6SL3300-7TE32-6AA1 [16]). The DC Link consists of the DCP (model IT6030C-80-900 [17]).

With respect to the drive branch, the components have been chosen by following the steps in the flowchart of Figure 7; in the case of the DCP branch, the selection procedure is indicated in Figure 8.

Using the half-shaft torque and speed profiles derived from Figure 10 as inputs, it is possible to compute the active and apparent powers absorbed at different points on the EOL test bench as a function of the test cycle time (once the selection of bench components is finalized and all the construction parameters of the various parts of the bench are defined).

The points corresponding to model parameters are shown in Figure 12; only the power values at the two branches' connecting point will be examined and contrasted with the actual measured values in the last section of this paper.

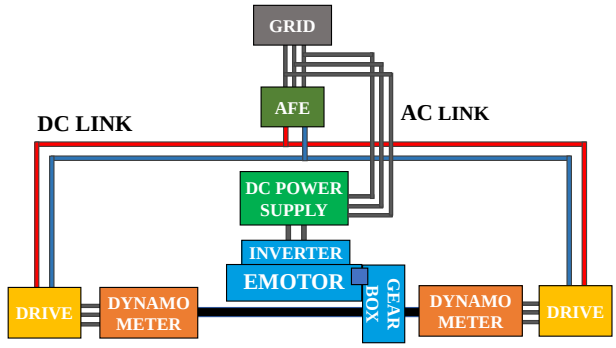

Figure 11. Connection diagram of the electrical power components of the bench with hybrid link configuration

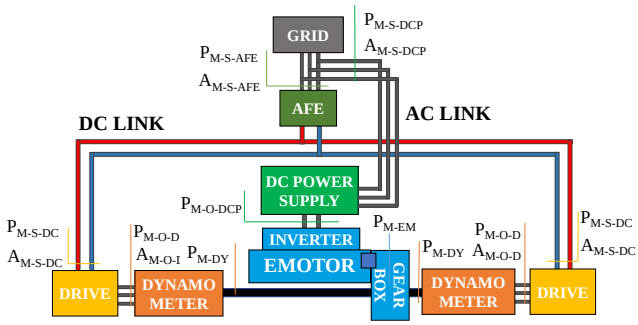

Figure 12. Power calculation points

In particular, $P_{M\text{-}S\text{-}AFE}$ from the drive branch and $P_{M\text{-}S\text{-}DCP}$ from the DCP branch will be taken into account, with the total power drawn from the plant grid P_{GRID} calculated as follows:

$$P_{GRID} = P_{M\text{-}S\text{-}AFE} + P_{M\text{-}S\text{-}DCP} \tag{26}$$

Figure 13 displays the power profiles for the drive branch (green line), the DCP branch (red line), and the total power needed by the plant (purple line). Positive values indicate that the power is absorbed by the system, while negative values indicate that the power is regenerated.

The dynamometers' and the e-axle's regeneration capabilities greatly affect the power needs. Thanks to the proper design of the EOL test bench, the peak power needed to test the e-axle without them is less than 40%. The model makes it possible even under dynamic testing situations with the e-axle operating points on the chosen components' operational maps. These working points are shown on the operational map of the chosen dynamometers in Figure 14. The blue line represents the maximum torque that can be produced when the e-axle operates under motor phase; on the other hand, the orange line represents the lowest point that can

be achieved during the e-axle's regeneration phase. Similarly, Figure 15 shows the operating points of the e-axle on the DCP map, with the highest current values achievable during the motor phase represented by the blue line and the maximum current values achievable in the regenerative phase corresponding to the orange line.

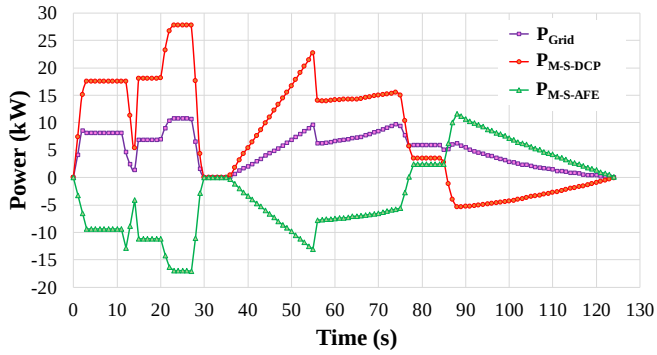

Figure 13. Power trends on both branches and total building absorption values

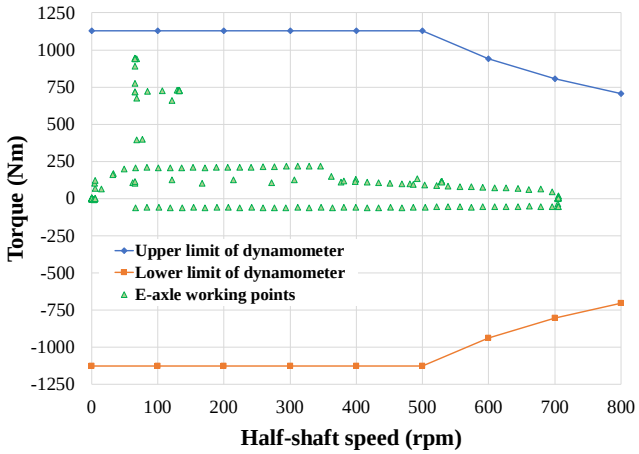

Figure 14. E-axle measured working points on dynamometer map

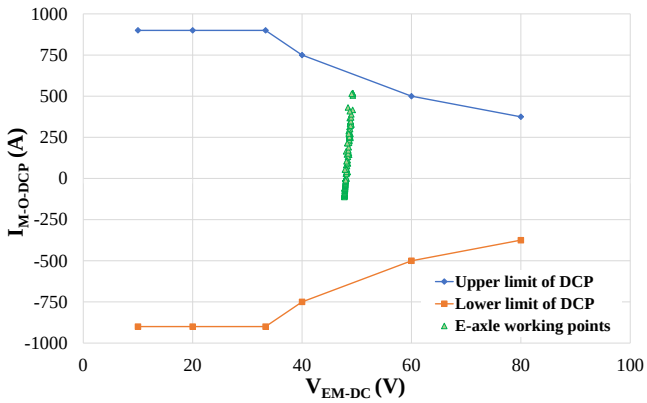

Figure 15. E-axle working points measured on DCP map

5. CONCLUSIONS

To optimize the design of an end-of-production-line (EOL) test bench for testing and certifying the functioning and performance of newly manufactured electric motors or axles for electric vehicles, a mathematical model has been developed. Based on this model, an EOL test bench has been designed to evaluate a low-power electric axle (approximately 22 kW). In the future, the model will be improved by incorporating the energy consumption of auxiliary equipment, such as pumps, PCs, servers, cooling units, and 12 V power supply. Additionally, dynamic modifications to efficiency and power factor of EOL test bench main components will be included in order to reduce differences between projected data and actual measured values. The accuracy of the model will be also assessed by contrasting the predicted data with experimental values derived from field tests.

REFERENCES

[1] Vidyanandan, K.V. (2018). Overview of Electric and Hybrid Vehicles. Energy Scan, 3: 7-14.

[2] Talari, K., Jatrothu, V.N. (2022). A review on hybrid electrical vehicles. Strojnícky Casopis - Journal of Mechanical Engineering, 72(2): 131-138. https://doi.org/10.2478/scjme-2022-0023

[3] López, I., Ibarra, E., Matallana, A., Andreu, J., Kortabarria, I. (2019). Next generation electric drives for HEV/EV propulsion systems: Technology, trends and challenges. Renewable and Sustainable Energy Reviews, 114: 109336. https://doi.org/10.1016/j.rser.2019.109336

[4] Chih-Hsien, Y., Chyuan-Yow, T., Chih-Ming, C. (2012). Study on power train of two axles four wheel drive electric vehicle. Energy Procedia, 14: 1528-1535. https://doi.org/10.1016/j.egypro.2011.12.1128

[5] Zhang, F.Q., Hu, X.S., Langari, R., Cao, D.P. (2019). Energy management strategies of connected HEVs and PHEVs: Recent progress and outlook. Progress in Energy and Combustion Science, 73: 235-256. https://doi.org/10.1016/j.pecs.2019.04.002

[6] Ma, C.B., Xu, M., Wang, H. (2011). Dynamic emulation of road/tyre longitudinal interaction for developing electric vehicle control systems. Vehicle System Dynamics, 49(3): 433-447. https://doi.org/10.1080/00423110903545172

[7] Itani, K., De Bernardinis, A., Khatir, Z., Jammal, A., Oueidat, M. (2016). Regenerative braking modeling, control, and simulation of a hybrid energy storage system for an electric vehicle in extreme conditions. IEEE Transactions on Transportation Electrification, 2(4): 465-479. https://doi.org/10.1109/TTE.2016.2608763

[8] Gautam, A.K., Tariq, M., Pandey, J.P., Verma, K., Urooj, S. (2022). Hybrid sources powered electric vehicle configuration and integrated optimal power management strategy. IEEE Access, 10: 121684-121711. https://doi.org/10.1109/ACCESS.2022.3217771

[9] Stock, T., Seliger, G. (2016). Opportunities of sustainable manufacturing in industry 4.0. Procedia CIRP, 40: 536-541. https://doi.org/10.1016/j.procir.2016.01.129

[10] Zhao, H., Li, C., Zhang, G.J. (2008). Design of a versatile test bench for hybrid electric vehicles. In 2008 IEEE Vehicle Power and Propulsion Conference, Harbin, China, pp. 1-4. https://doi.org/10.1109/VPPC.2008.4677463

[11] Zhao, W.B., Song, Q., Liu, W.B., Ahmad, M., Li, Y.T. (2019). Distributed electric powertrain test bench with dynamic load controlled by neuron PI speed-tracking method. IEEE Transactions on Transportation

Electrification, 5(2): 433-443. https://doi.org/10.1109/TTE.2019.2904652
[12] Cardone, M., Gargiulo, B., Fornaro, E. (2021). Development of a flexible test bench for a hybrid electric propulsion system. In 2021 IEEE International Workshop on Metrology for Automotive (MetroAutomotive), Bologna, Italy, pp. 221-225. https://doi.org/10.1109/MetroAutomotive50197.2021.9502723
[13] Lo Bianco, G., Pede, G., Puccetti, A., Rossi, E., Mantovani, G. (2001). Vehicle testing in ENEA drive-train test facility. In SAE 2001 World Congress, pp. 101-111. https://doi.org/10.4271/2001-01-0961
[14] Assing S.p.A. The research partner. https://www.assing.it/, accessed on Jun. 17, 2024.
[15] Siemens SIMOTICS M-1PH8 Induction Motors Data Manual. (2022). Siemens Inc., Munich, Germany, pp. 32-789. https://support.industry.siemens.com/cs/attachments/109808406/1PH8_config_man_tdc_asynchron_1222_en-US.pdf?download=true, accessed on Jun. 17, 2024.
[16] Siemens Motion Control Drives SINAMIC S120 e SIMOTICS Data Manual. (2017). Data Manual, pp. 61-365. https://cache.industry.siemens.com/dl/files/019/109747019/att_918079/v1/motion-control-drives-D21-4-complete--Italian-2017.pdf, accessed on June 17, 2024.
[17] ITECH - IT6000C Series Bidirectional Programmable DC Power Supply Data Manual (2023). ITECH Electronic Co., Ltd., New Taipei, Taiwan, pp. 2-7. https://www.calpower.it/gallery/cpit6000c-en-2021826.pdf, accessed on Jun. 17, 2024.